*Physicochem. Probl. Miner. Process., 61(2), 2025, 203078*

http://www.journalssystem.com/ppmp

Physicochemical Problems of Mineral Processing

ISSN 1643-1049


# Effect of sodium diethyldithiocarbamate (DDTC) and xanthate collaborative collection in malachite sulfurization flotation: Enhancement and mechanisms

**Ayman M. Ibrahim [1,2], Han Wang [1], Gar Elnabi [2], Jaber A. Yousif [3], Haiyang He [1], Dianwen Liu [1]**

[1] State Key Laboratory of Complex Nonferrous Metal Resources Clean Utilization, Yunnan Key Laboratory of Green Separation and Enrichment of Strategic Metal Resources, Faculty of Land Resources Engineering, Kunming University of Science and Technology, Kunming 650093 Yunnan, PR China

[2] Department of Mining Engineering, University of Nyala, Nyala, South Darfur 63311, PR Sudan

[3] Department of Mining Engineering, Faculty of Engineering, Eldaein University, Eldaein 63312, Sudan

Corresponding authors: wanghankmust@126.com (H. Wang), dianwenliu1@kust.edu.cn (D. Liu)

**Abstract:** This study investigates the enhancement of malachite flotation using sodium diethyldithiocarbamate (DDTC) and xanthate as collectors in combination with sodium sulfide ($Na_2S$). Both collectors promote adsorption on the malachite surface, aiding in forming a copper sulfide (Cu–S) layer that increases surface hydrophobicity and enhances surface roughness, further improving reagent adsorption. $Na_2S$ also stabilizes the Cu–S layer, optimizing flotation performance. Under optimal pH conditions, the combined treatment of $Na_2S$ with DDTC and xanthate achieved the highest flotation recovery (93.15%), outperforming traditional methods. This treatment shifted the malachite contact angle from hydrophilic to hydrophobic, and its zeta potential became increasingly negative. DDTC and xanthate adsorb onto the positively charged copper species through their dithiocarbamate and xanthate ion groups (R-O-C=S−). XPS and FTIR analyses reveal that $Na_2S$ interacts with copper ions, reducing $Cu^{2+}$ to $Cu^{+}$, while DDTC enhances the stability of the copper sulfide layer on the malachite surface. FESEM-EDS analysis shows that the activation products evolved from small aggregate films to dense, cloud-like layers with sulfide deposits, reflecting dynamic surface changes. Flotation experiments demonstrate that DDTC and xanthate improve sulfurization performance, significantly enhancing malachite flotation. These findings indicated that both collectors increased the recovery and provided valuable insights into malachite sulfurization mechanisms.

***Keywords:*** sodium diethyldithiocarbamate (DDTC), sulfurization flotation, collector, malachite, enhancement

## 1. Introduction

Copper oxide ores have been a critical resource for centuries and continue to play an essential role in meeting global copper demand (Arndt et al., 2017; Rötzer and Schmidt, 2020). These ores contain various copper oxide minerals, including malachite, azurite, cuprite, and tenorite (Chávez Jr, 2021; Zhang et al., 2020). With projections for increased industrialization, construction, and electrical manufacturing, alongside evolving environmental regulations, copper oxide consumption is expected to rise (Agrawal and Sahu, 2010; Grozdanka D. Bogdanović, Velizar D. Stanković, Maja S. Trumić, Dejan V. Antić, 2016; Majumdar and Ghosh, 2021; Northey et al., 2014). Malachite is a significant oxidized copper mineral that displays high hydrophilicity due to surface hydroxyl groups, leading to poor collection efficiency with traditional sulfide copper collectors (JIA et al., 2023; Lu et al., 2023; Wu et al., 2017). Without pretreatment, effectively enriching malachite is challenging. The traditional sulfurization-xanthate flotation technique is the most widely used method for recovering malachite. During this process, the addition of a sulfurizing agent reacts with the oxidized mineral surface, forming

DOI: 10.37190/ppmp/203078

a metal sulfide layer that increases surface reactivity. Feng et al. (2017) found that several cuprous sulfide species, including cuprous monosulfide, disulfide, and polysulfide, formed on the malachite surface during sulfurization-xanthate flotation. The concentration of these species increased with sodium sulfide concentration, enhancing surface reactivity. However, the effectiveness of sulfurization flotation is strongly influenced by the amount of $Na_2S$ used. The extraction of valuable components from malachite-bearing ores is complex due to the need to separate malachite from gangue and clay minerals, which requires a combination of physical and chemical methods and careful selection of extractive techniques (Liu et al., 2018; Wang et al., 2022). Using sodium sulfide as a sulfurizing reagent in copper oxide flotation has proven effective in enhancing the recovery of copper oxide minerals (Ibrahim et al., 2023, 2022; Maleki et al., 2023; Xue et al., 2023). During the flotation process, copper sulfide is the primary sulfide product formed on the malachite surface. This copper sulfide forms through a growth process, meaning that brief sulfide treatment results in a smaller amount of newly formed sulfide on the malachite surface. The newly formed copper sulfide is unstable when adsorbed onto the mineral surface and may detach during mechanical stirring. As the duration of sulfide treatment increases, more copper sulfide particles detach. The stability of the sulfide layer must be carefully controlled, as both excessive and insufficient sulfide treatment can negatively impact copper recovery (Bai et al., 2020; Feng et al., 2017; Li et al., 2018). Ongoing research aims to optimize process conditions and understand the underlying mechanisms of the sulfurization reaction.

Due to the hydrophilic nature of copper oxide minerals, flotation can be challenging and often requires specific reagents. Common collectors include xanthates, dithiophosphates, and thionocarbamates (Li et al., 2015, 2025; Liu et al., 2019). The recovery of copper minerals requires collectors to enhance the process, with the most popular collectors being xanthates, dithiophosphates, fatty acids, and thiocarbamate, all of which have divergent effects on copper mineral surfaces. Xanthates are particularly popular because of their strong affinity for copper sulfide minerals and their effectiveness in alkaline environments (Mustafa et al., 2004; Zhang et al., 2013). The sulfurization-xanthate flotation system is an alternative to the DDTC-sulfurization flotation system. It involves sulfurizing copper oxide minerals and then collecting them using xanthate. Chen et al. (2025) found that adjusting sodium sulfide concentrations could control malachite's surface hydrophobicity and improve recovery. Dithiophosphates are preferred for their selective adsorption in complex ore systems, while dithiocarbamates form stable metal-dithiocarbamate complexes, which are advantageous in specific flotation conditions (Gupta et al., 2015, 2013). Thionocarbamates are less commonly used, but they have shown potential in specific flotation applications, especially for copper oxide ores. Although the individual impacts of xanthates and sodium diethyldithiocarbamate (DDTC) on copper oxide flotation have been investigated, only a few studies have focused on their combined effects. Some research suggests that DDTC, as a mixed collector, can improve flotation performance by modifying surface properties and potentially enhancing recovery (Liao et al., 2024). Furthermore, the interaction between DDTC and xanthates may influence flotation kinetics, including bubble-particle attachment, surface charge, and froth stability. Further studies on these combined effects could offer valuable insights for optimizing flotation processes for copper oxide minerals. In previous studies, McFadzean et al. (2015) also investigated the heat produced during reactions between sodium ethyl xanthate, sodium isobutyl dithiocarbamate, and their mixtures with chalcopyrite and pyrite, using an isothermal titration microcalorimeter.

Therefore, this study aims to investigate and optimize the performance of sodium diethyldithiocarbamate (DDTC) as a collector in combination with xanthate during the sulfurization flotation of malachite. Flotation tests were carried out to evaluate the effect of operating parameters, including pH, time, and concentrations of both DDTC and xanthate collectors. Additionally, various techniques, including X-ray photoelectron spectroscopy (XPS), ultraviolet spectroscopy (UV), atomic force microscopy (AFM), field emission scanning electron microscopy-energy dispersive spectroscopy (FESEM-EDS), contact angle measurements, Zeta potential measurements, fourier transform infrared spectroscopy (FT-IR), adsorption experiments, were employed to investigate the impact of DDTC on the surface properties and sulfurization response of malachite. This work provides new insights into the collection mechanism of malachite sulfurization flotation under cationic–anionic collector conditions.

## 2. Experimental

### 2.1. Materials and reagents

Malachite samples were sourced from Kunming, Yunnan Province, China. As shown in Table 1, the malachite sample analysis revealed the following composition: Cu 56.14%, Mn 0.40%, Fe 0.10%, $SiO_2$ 2.32%, $Al_2O_3$ 0.56%, CaO 0.70%, MgO 0.32%, and other elements 39.46%. The bulk malachite samples were crushed and hand-pulverized. After initial crushing, the sample was ground in a ball mill to reduce the particle size further by using screens. The three types of powder, with particle sizes ranging from −74 to +38 μm, were used in micro-flotation, FTIR, and XPS analyses. For other tests, the blocky samples were cored into cubes of a regular geometry and then processed for Atomic Force Microscopy (AFM) analysis and Time-of-Flight Secondary Ion Mass Spectrometry (ToF-SIMS) characterization. NaOH and HCl were used in the present investigation to control the pH. All the reagents used in this study were analytical grade, and deionized (DI) water was used.

Table 1. XRF analysis of major elements in the sample

| Elements | Cu | Mn | Fe | $SiO_2$ | $Al_2O_3$ | CaO | MgO | Others |
|---|---|---|---|---|---|---|---|---|
| **Wt. (%)** | 56.14 | 0.40 | 0.40 | 2.32 | 0.56 | 0.70 | 0.32 | 39.46 |

### 2.2. Flotation study

The micro-flotation experiments were carried out using an XFG flotation machine. Pure malachite samples were collected, crushed, and ground to achieve a particle size range of −74 to +38 μm. As needed, fresh concentrations of DDTC and $Na_2S$ were prepared, along with other reagents, including pH modifiers (NaOH or HCl), frothers (methyl isobutyl carbinol), and additional surfactants. Initially, 2 g of the malachite sample was mixed with 36 $cm^3$ of deionized water, along with the appropriate pH regulators and reagents, and stirred in the flotation cell for five minutes, as illustrated in Fig. 1. Finally, the concentrate and tailings were collected, dried, and weighed to evaluate the flotation recovery percentage of the malachite using Equation (1).

$$\varepsilon = \frac{m_1}{m_1+m_2} \times 100\% \quad (1)$$

Here, $\varepsilon$ represents recovery, and $m_1$ and $m_2$ denote the masses of the foam and tailing products, respectively.

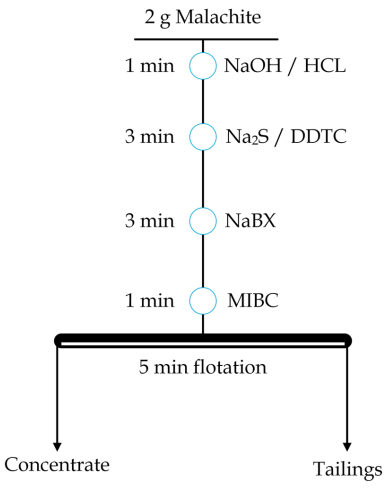


Fig. 1. Flowsheet of the micro-flotation tests

### 2.3. XPS study

X-ray photoelectron spectroscopy was performed to analyze the effect of collaborative collection collectors of DDTC and NaBX on sulfurized malachite surfaces. The XPS was analyzed using a PHI 5000 spectrometer (Japan) with an Aluminium Kα X-ray source, 1486.6 eV. Spectra were collected across the binding energy range to identify key elements and their states and achieve a high spectral resolution of

the Cu $2p_{3/2}$ and S 2p core-level regions. Malachite was conditioned with DDTC and $Na_2S$ solutions at the optimal concentration determined from previous flotation tests. The samples used in the tests were prepared as in the FTIR and flotation experiments.

### 2.4. UV spectroscopy study

The UV-Vis analysis of malachite samples was performed using UV-Vis spectroscopy (UVProbe 3600). For sample preparation, 2 g of malachite was suspended in 36 ml of deionized water. DDTC and $Na_2S$ were added sequentially to the reaction, with reaction times varying at 0, 5, 10, 15, and 20 minutes, using a constant concentration ratio of DDTC and $Na_2S$. After stirring and allowing the mixture to settle for 30 seconds, 10 ml of the clear supernatant was delivered into a centrifuge tube. The centrifugation was set at 2200 rpm for 40 mins, after which 3ml of the supernatant was taken for testing.

### 2.5. AFM study

AFM was used to determine malachite's surface morphology and crystallization features before and after DDTC and sodium sulfide treatment. Scanning was performed using a Dimension Icon AFM from Bruker (United States). The pure cubic malachite samples were placed directly into a glass beaker, and deionized (DI) water (18.25 mΩ·cm) was added to the solution, adjusting the pH to around 9. Depending on the experimental conditions, fresh solutions of DDTC and $Na_2S$ were prepared and added, and then the samples were modified for 10 minutes. After conditioning, the samples' surfaces were dried in a vacuum oven before the AFM analysis.

### 2.6. FESEM-EDS study

The sample analysis was conducted to describe the surface morphology and perform an elemental analysis of malachite after treatment with DDTC and $Na_2S$. The elements analyzed included Cu, O, C, and S, using a surface analysis method with EDS. The sample preparation steps were as follows: A portion of the sample was treated with the reagent solutions and then washed. The treated samples were placed in a vacuum dryer and coated with platinum before performing an SEM-EDS scan for analysis.

### 2.7. Contact angle study

The contact angle measurements (CA) were made using a JY−82B (Dingsheng) instrument. The samples were polished with $Al_2O_3$ sandpaper (500 grit and 4000 grit) under different setting conditions. After cleaning, the malachite was placed in a beaker containing 50 mL of deionized water. Following the flotation test protocol, the required reagents were added sequentially, with each reagent allowed to react with the minerals for 5 minutes. After the reagent reaction, the mineral sample was placed in a contact angle measurement instrument. Images of the water droplet shape were captured with a camera and analyzed using ImageJ 1.46r (National Institutes of Health, Wayne Rasband, United States) and saved. Each condition was tested at least twice to ensure the accuracy of the contact angle measurements.

### 2.8. Zeta Potential study

The zeta potential of malachite samples was measured using a Malvern Zetasizer (United Kingdom), which utilizes laser Doppler electrophoresis to assess the electrokinetic potential of particles in suspension. Fresh solutions of $2 \times 10^{-3}$ mol/dm³ $Na_2S$ and $1 \times 10^{-4}$ mol/dm³ NaBX were prepared for the experiment. Following the outlined procedure, a 0.5 g sample of malachite (−47 µm) was used. The pH was adjusted by adding NaOH or HCl to achieve the desired value. A $1 \times 10^{-3}$ mol/dm³ KCl electrolyte was also prepared. After approximately 5 minutes, the fine particles settled, and the supernatant was transferred to a specialized container for measurement. Each sample was measured three times, and the average value was used for the final result.

### 2.9. FT-IR study

FTIR experiments were conducted using a Nicolet iS50 from Thermo Nicolet Corporation (USA). For FTIR analysis, 2 grams of the mineral sample, with particles finer than 74 µm, were added to deionized water in a volumetric flask and stirred. NaOH and HCl solutions were then used to adjust the pH to around 9. Sodium diethyldithiocarbamate (DDTC) and (NaBX) were freshly prepared for sulfurization.

After 10 minutes of stirring, the malachite samples were filtered and vacuum-dried at approximately 40 °C. Finally, at room temperature, FTIR spectra were recorded from 400 to 4000 $cm^{-1}$ for each reagent and mineral.

## 3. Results and discussion

### 3.1. Flotation analysis

Fig. 2 shows the effects of initial DDTC and NaBX as collectors, $Na_2S$ concentrations, pH, and flotation time on malachite recovery. The floated response of malachite to (DDTC $2 \times 10^{-3}$ mol/$dm^3$) and ($Na_2S$ $2 \times 10^{-3}$ mol/$dm^3$) was also investigated at varying pH of 5, 6, 7, 8, 9, 10, and 11. As the pH increased from 5.0 to 11.0, the recovery progressively improved. Under optimal pH conditions, DDTC exhibited moderate collection efficiency, peaking at 33.24% at pH 9.0 and then declining to 19% at pH 11. On the other hand, $Na_2S$ had better collection efficiency, achieving a maximum recovery of 49.27% at pH levels 9 and maintaining 41.3% at pH 11. The combined application of both collectors with sodium sulfide at the same pH yielded the highest collection efficiency, with a peak recovery of 93.15%. However, as pH levels exceeded 9, the total malachite recovery tended to decrease, reaching a maximum of 68.15% at pH 11, indicating an increased probability of undesirable chemical changes, such as surface deactivation and decreased efficacy of flotation reagents, as depicted in Fig. 2(a). Similarly, as flotation time increased from 1 to 10 minutes, the flotation recovery of malachite improved by 30.40% and 43.15% with DDTC, NaBX, or $Na_2S$ treatments, respectively. Under the same conditions, the sample treated with $Na_2S$ and a combination of DDTC and xanthate exhibited improved collection performance, achieving a higher flotation recovery of 93.46%, as shown in Fig. 2(b).

When flotation time exceeded 20 minutes, all recovery slightly increased before stabilizing. This indicates that the mechanical energy applied to keep particles in suspension (such as agitation or aeration) may become less effective at longer flotation times, further slowing the recovery rate.

Fig. 2(c) illustrates the effect of $Na_2S$ concentration, ranging from $5 \times 10^{-4}$ to $3.5 \times 10^{-3}$ mol/$dm^3$, on the floatability of malachite. Malachite recovery rose from 27.48% to 52.95%, with an improvement in the concentration range of $5 \times 10^{-4}$ to $1.5 \times 10^{-3}$ mol/$dm^3$. However, as the $Na_2S$ concentration increased

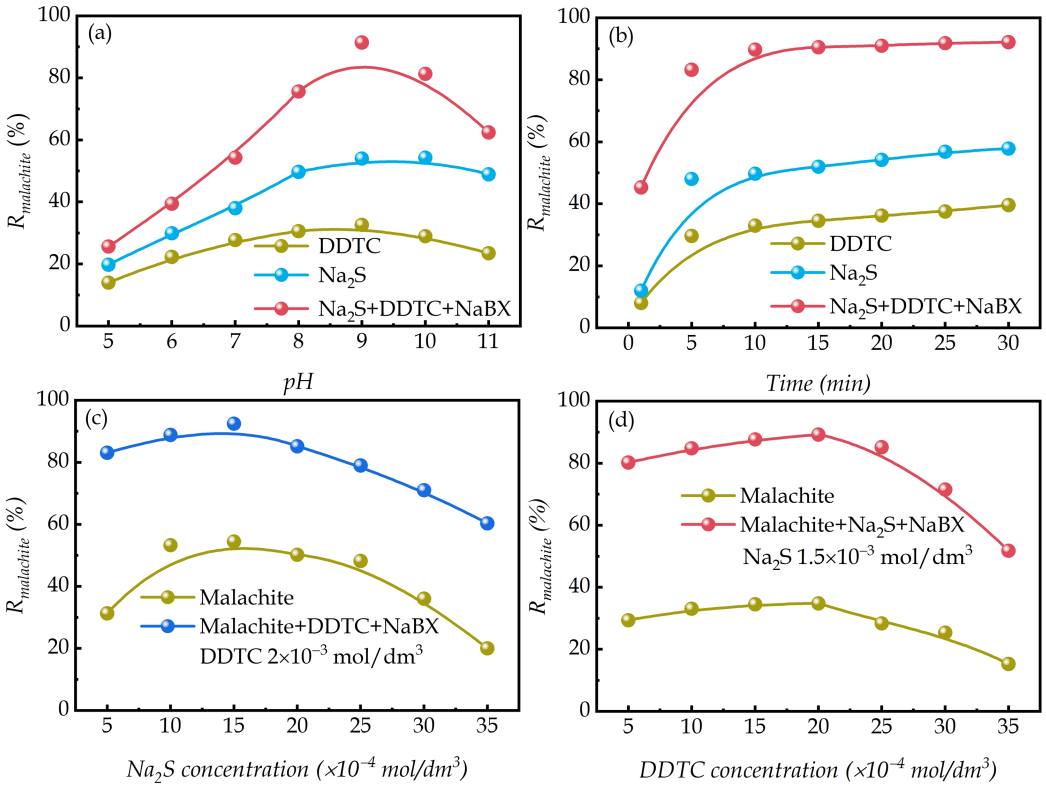


Fig. 2. Malachite flotation recoveries across varying conditions: (a) pH, (b) time, (c) $Na_2S$ concentration, and (d) DDTC concentration, NaBX=$1 \times 10^{-4}$ mol/$dm^3$

from 1.5 × $10^{-3}$ to 3.5 × $10^{-3}$ mol/dm$^3$, the recovery rate sharply decreased from 76.7% to 34.8% at 3.5 × $10^{-3}$ mol/dm$^3$. When treated with DDTC and xanthate at the same $Na_2S$ concentrations, the maximum recovery observed was 91.27%. Conversely, the efficiency of malachite recovery decreased as the concentration of the solution increased because the adsorption of an insoluble salt precipitate, originating from the reaction of $Na_2S$ and dissolved Cu ions, occurred. This reaction effectively restores the surface's hydrophilic nature, thereby reducing floatability (Li et al., 2025).

Fig. 2(d) illustrates the effect of DDTC concentration on malachite floatability. A positive correlation between DDTC or xanthate concentrations and malachite recovery is observed. Within the DDTC concentration range of 5 × $10^{-4}$ to 2 × $10^{-3}$ mol/dm$^3$, the highest recovery obtained was 31.55% at 2 × $10^{-3}$ mol/dm$^3$. However, as the DDTC concentration rose beyond this point, recovery dropped to as low as 17.6% at 3.5 × $10^{-3}$ mol/dm$^3$, likely due to unwanted reactions, such as precipitate formation, which disrupted the flotation and separation processes. The results indicate that DDTC demonstrates high collection efficiency at similar concentrations in treatments with malachite and $Na_2S$-NaBX, achieving maximum recovery of 88.4%. However, with an increase in DDTC concentration to 3.5 × $10^{-3}$ mol/dm$^3$, malachite recovery decreased to 56.36%.

### 3.2. XPS analysis

XPS analysis was applied to study the surface compositions of malachite in both the presence and absence of DDTC and sodium sulfide ($Na_2S$). The resulting spectra and detailed surveys of copper (Cu) and sulfur (S) are presented in Fig. 3. The binding energies of Cu 2p3/2 in the pure mineral appeared at 935.02 eV, as depicted in Fig. 3(a). The pure malachite surfaces exhibit spin-orbit split peaks, which can be ascribed to the divalent copper ($Cu^{2+}$) component present on the malachite surfaces (Feng et al., 2018). Following DDTC treatment, the binding energy peaks for Cu 2p3/2 were identified as two distinct components located at approximately 932.25 eV and 934.14 eV, as illustrated in Fig. 3(b). These peaks correspond to copper in the +1 (Cu(I)) and +2 (Cu(II)) species, respectively. The analysis revealed that a notable portion of Cu(II) was converted to Cu(I), with Cu(I) and Cu(II) accounting for 63.23% and 36.77%, respectively. This observation indicates that DDTC minimally impacts the overall copper composition in minerals. When malachite was treated with $Na_2S$ (Fig. 3(c)), the Cu 2p3/2 peak revealed two distinct components at binding energies of 932.27 eV and 934.73 eV, indicating the sulfurization of the malachite surface by $Na_2S$ (Ibrahim et al., 2025; Zhang et al., 2022). The total copper content was measured at 56.49% Cu(II) and 43.51% Cu(I). This observation indicates that $Na_2S$ changes the electronic environment of copper on the mineral surface, resulting in an increased proportion of Cu(I) and a corresponding decrease in Cu(II). In contrast, after treating malachite with $Na_2S$ and DDTC, the results shown in Fig. 3(d) indicate that the Cu 2p3/2 peaks correspond to binding energies of 932.37 eV and 934.75 eV. The total copper content was approximately 30.38% for Cu(II) and 69.62% for Cu(I), associated with Cu–S and Cu–O bonds, respectively (Xiao et al., 2024). This indicates that a substantial portion of Cu(II) was converted to Cu(I) species, as DDTC acts as a reagent facilitating the reaction between sulfur and copper ions. This interaction forms a protective copper sulfide (Cu–S) layer on the mineral surface, improving malachite's stability and its reactivity in chemical processes.

The S 2p XPS spectrum shows that 2p orbital elements in the 2p1/2 and 2p3/2 states exhibit similar chemical properties, leading us to focus on the S 2p3/2 spectrum. This results in pairs of spectral lines appearing due to the electron's spin and orbital motion interaction. As illustrated in Fig. 3(e), no binding energy peak for sulfur is detected in pure malachite, confirming the absence of sulfur species and indicating the sample's purity, with no contaminating sulfide or sulfonate species present. Following malachite post-treatment with DDTC (Fig. 3(f)), the S 2p spectrum splits into two distinct peaks. These peaks are located at binding energies of 162.55 eV and 164.18 eV (S 2p3/2) and account for approximately 58.96% and 41.04% of the total sulfur content, respectively, corresponding to the $S^{2-}$ and $S_n^{2-}$ species. This result indicates that sulfur underwent oxidation during the DDTC modification, which is beneficial for enhancing the mineral's activation.

When the pure malachite was treated with ($Na_2S$), the S 2p3/2 spectrum was fitted to reveal three spectral peaks at binding energies of 162.69 eV, 164.25 eV, and 168.97 eV, corresponding to the $S^{2-}$, $S_n^{2-}$, and $SO_n^{2-}$ fractions, with proportional percentages to 44.60%, 46.91%, and 8.49%, respectively. The percentage of $S^{2-}$ species likely corresponds to sulfur species adsorbed onto the surface, while the $S_n^{2-}$

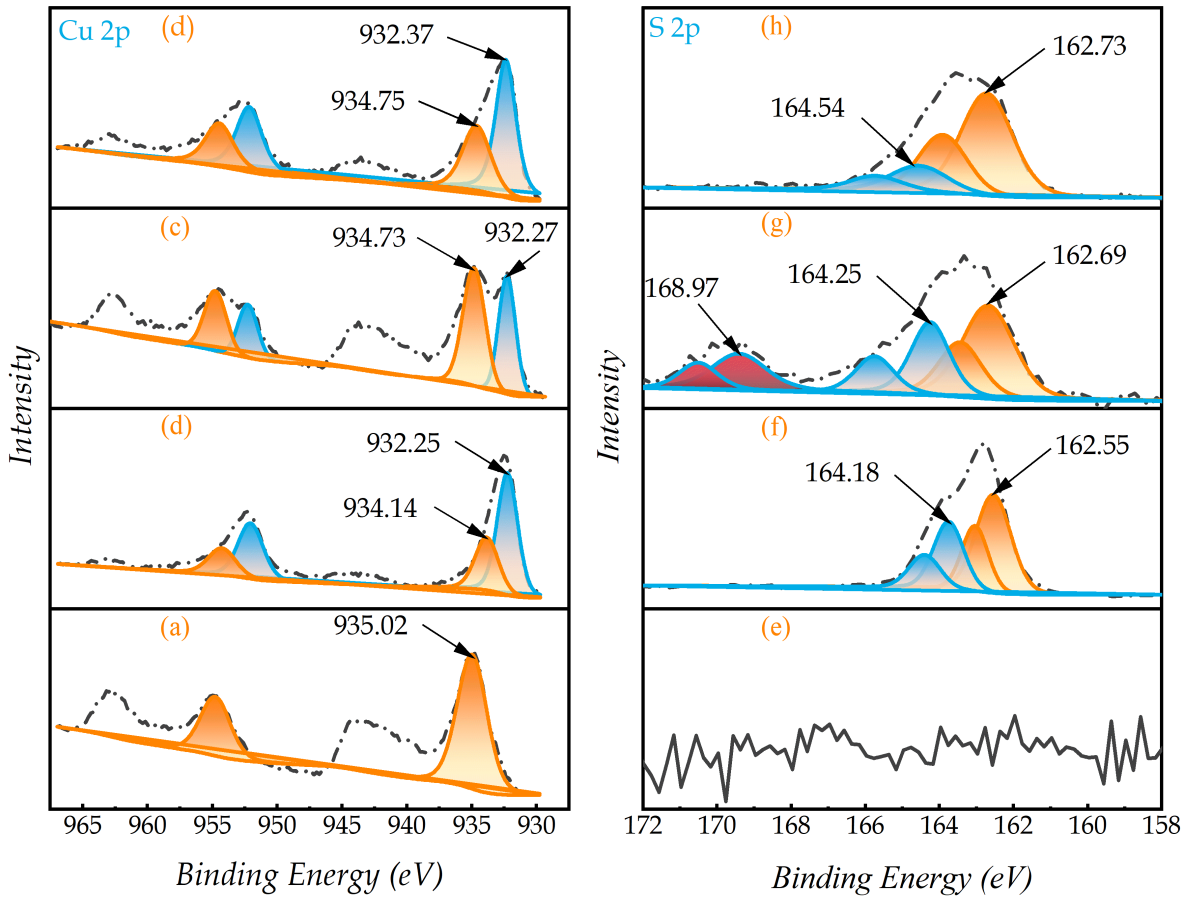


Fig. 3. High-resolution XPS Cu 2p and S 2p spectra of (a, e) pure malachite, after (b, f) DDTC treatment, after (c, g) $Na_2S$ treatment, and after (d, h) $Na_2S$+ DDTC treatment.

species may indicate a minor oxidation process that enhances the surface reactivity of the sample. In contrast, the presence of $SO_n^{2-}$ species suggests excessive oxidation of the sulfurization products, which leads to reduced surface reactivity, as illustrated in Fig. 3(g) (Gupta et al., 2013; Ibrahim et al., 2023).

After adding $Na_2S$ and DDTC, the peak at approximately 162.73 eV is attributed to the $S^{2-}$ fraction, while the peak at around 164.54 eV corresponds to the $S_n^{2-}$ fraction. This division into two peaks indicates the presence of sulfide ions and polysulfides, reflecting the distinct chemical environments of sulfur on the modified surface, and does not result in more oxidized $SO_n^{2-}$ species. Compared to sulfurized malachite, the percentage of $S^{2-}$ decreased by 1.42%, while the percentage of $S_n^{2-}$ increased by 3.91%, as shown in Fig. 3(h). The decrease in $S^{2-}$ content is attributed to slight oxidation on the mineral surface, which enhances the reactivity of the malachite. This change may result from a strong frontal redox reaction between $Cu^{2+}$, DDTC, and $Na_2S$, forming more copper-sulfur species. In contrast, the increase in $S_n^{2-}$ indicates that sulfur species were oxidized at the malachite surface. This phenomenon demonstrates that the malachite surface is undergoing chemical transformations that likely enhance its reactivity.

### 3.3. UV spectra analysis

UV–visible spectroscopy was applied to study the time-dependent absorption spectra, revealing the adsorption dynamics of compounds on mineral surfaces across changes in absorbance, peak positions, and new spectral features. Of all the models used in UV–visible optical spectroscopy, the Tauc plot method is one of the most effective and easiest to apply (Nikitha et al., 2024). Fig. 4 illustrates the UV–vis spectra of the malachite flotation solution treated with DDTC and $Na_2S$ over time. Two absorption peaks of DDTC are observed at wavelengths of 257 nm and 282 nm (Téllez S. et al., 2016). The first peak at 257 nm exhibits intensities of 5.51, 4.88, 4.51, 4.25, and 3.34, measured after 0, 5, 10, 15, and 20 minutes of adsorption, respectively. Simultaneously, the second peak at 282 nm shows intensities of 5.21, 4.74,

4.44, 4.18, and 3.28, respectively. According to the obtained results, the absorbance of DDTC is inversely proportional to the UV exposure time. Therefore, due to the photodegradation of the DDTC molecule, prolonged UV exposure led to its photochemical breakdown, causing it to undergo photolysis—a chemical breakdown induced by photon absorption.

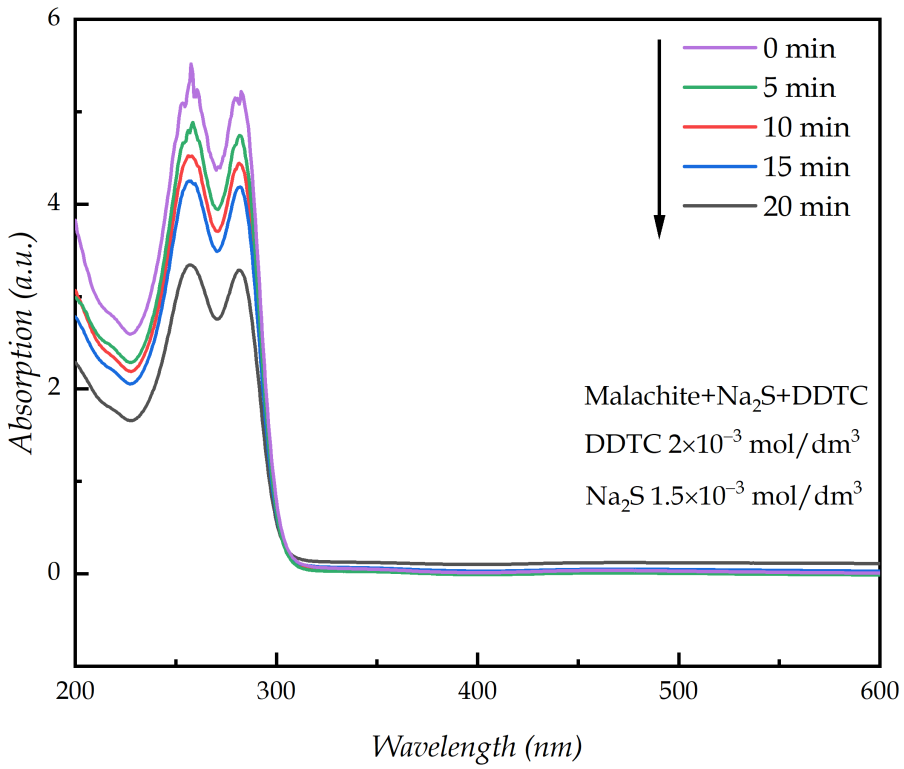


Fig. 4. UV–vis spectra of the flotation solution modified with DDTC and sodium sulfide as a function of time, pH 9±0.1

### 3.4. Surface roughness and morphology of malachite

Atomic force microscopy effectively characterizes surfaces, particularly in assessing reagent adsorption on mineral surfaces, regardless of the sulfurization process. The 2D and 3D topographies obtained from AFM provide insights into mineral surface morphology, revealing variations in both topography and height, as depicted in Fig. 5 (Dong et al., 2021; Yu et al., 2023). The atomic force microscopy (AFM) analysis of pure malachite revealed distinct surface features that characterize its morphology. The AFM images of polished malachite demonstrate a relatively smooth surface with well-defined crystalline structures. Fig. 5(a, b) presents the 2D images, cross-sectional height diagram, and 3D representations of malachite, revealing a surface roughness of approximately 5.99 nm. These results support the claim that the malachite surface is clean and pure without undergoing any additional processing. When malachite was treated with DDTC (Figs. 5(c, d)), new surface structures formed, and the mean roughness increased to 13.47 nm compared to pure malachite. This result indicates slight DDTC adsorption on the surface. Following the treatment of malachite with sodium sulfide (Figs. 5(e, f)), the intensity, as well as the number of the peak values in the 3D image height topography, evidence the adsorption of formed sulfide products on the malachite surface (Ibrahim et al., 2025; Zuo et al., 2024). The malachite roughness increased by 10.69 nm (Ra) compared to the pure mineral, suggesting that only a tiny quantity of sulfide products was adsorbed onto the modified surface.

In contrast, Figs. 5(g, h) illustrates the morphology of malachite treated with both DDTC and $Na_2S$, showing an increased number and height of columnar protrusions on the surface. The mean roughness of 22.36 nm was greater than that of malachite treated with either DDTC or $Na_2S$ alone, indicating that adsorption was enhanced when DDTC was applied prior to sodium sulfide treatment. This finding aligns with the FESEM-EDS analysis, which demonstrated that using DDTC as a collector improved the flotation recovery of malachite.

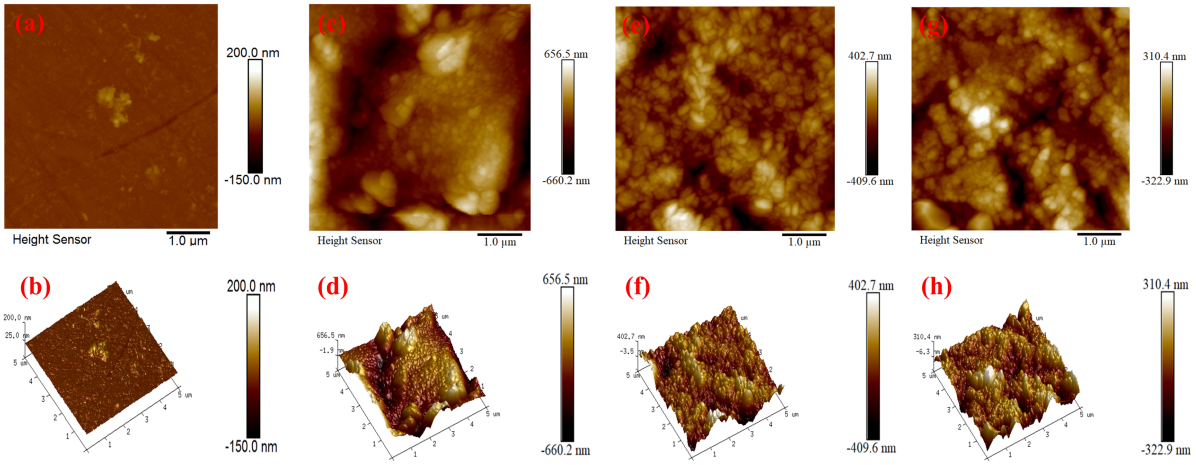


Fig. 5. Surface roughness and morphology of (a, b) pure malachite, (c, d) DDTC treatment, (e, f) $Na_2S$ treatment, and (g, h) $Na_2S$ + DDTC treatment

### 3.5. FESEM-EDS Analyses

FESEM-EDS analysis was conducted to examine the morphology of sulfurized malachite, both with or without DDTC as a collector, as shown in Fig. 6. The surface of pure malachite appeared smooth and uniform from the exterior, displaying subtle textural variations inherent to its natural morphology. Elemental analysis revealed prominent peaks for Cu, O, and C with concentrations of 53.7%, 30.1%, and 16.2%, respectively, presented in Figs. 6(a, b). After DDTC treatment, small aggregates of a white film formed on the surface, indicating slight interaction between DDTC and malachite, as seen in Figs. 6(c, d). This film may enhance surface reactivity by modifying adsorption characteristics for subsequent processing. EDS analysis showed a surface composition of 48.1 wt.% Cu, 32.5 wt.% O, and 15.3 wt.% C. In contrast, after treatment with sodium sulfide, the surface morphology exhibited irregular films identified as sulfide deposits (Liu et al., 2024; R. Liu et al., 2020). EDS analysis revealed weight percentages of 45.7% Cu, 38.8% O, 14.9% C, and 0.6% S, confirming the presence of sulfur within these attachments, as shown in Figs. 6(e, f). Compared to DDTC treatment, sodium sulfide was more effective in enhancing malachite flotation performance, as indicated by the small amount of sulfur detected on the mineral surface.

Figs. 6 (g, h) show the surface characteristics of malachite after treatment with $Na_2S$ and DDTC. The activation products evolved from small aggregate films to dense cloud layers, indicating dynamic changes in the activation process. EDS analysis showed that Cu and O distribution percentages decreased to 44.5% and 27.5%, respectively, while the weight percentages of C and S increased by 10.1% and 1.7%, respectively, compared to direct sulfurization. These results suggest that the DDTC collector actively promotes the formation of additional sulfide layers on the malachite surface.

### 3.6. Contact angle analysis

Fig. 7 shows pure malachite's contact angle (CA) measurements under various treatments. Untreated malachite exhibited a contact angle of 67.7° (Fig. 7(a)), indicating a hydrophilic surface that cannot float. With malachite treated with DDTC, the contact angle increased to 71.77° (Fig. 7(b)), suggesting moderate hydrophobicity. When treated with sodium sulfide, the contact angle rose to 76.78° (Fig. 7(c)), indicating a change in surface wettability and the formation of a copper sulfide layer that made the surface more hydrophobic than with DDTC alone. After treatment with $Na_2S$ + DDTC + NaBX, the contact angle increased significantly to 97.12° (Fig. 7(d)), reflecting a substantial shift toward hydrophobicity. This change demonstrates that DDTC and NaBX promote the creation of a less polar, more hydrophobic surface, thereby significantly improving malachite's hydrophobicity and optimizing mineral separation. According to previous studies by Zafar Said, a surface is considered hydrophobic when the contact angle exceeds 90° (Said et al., 2022).

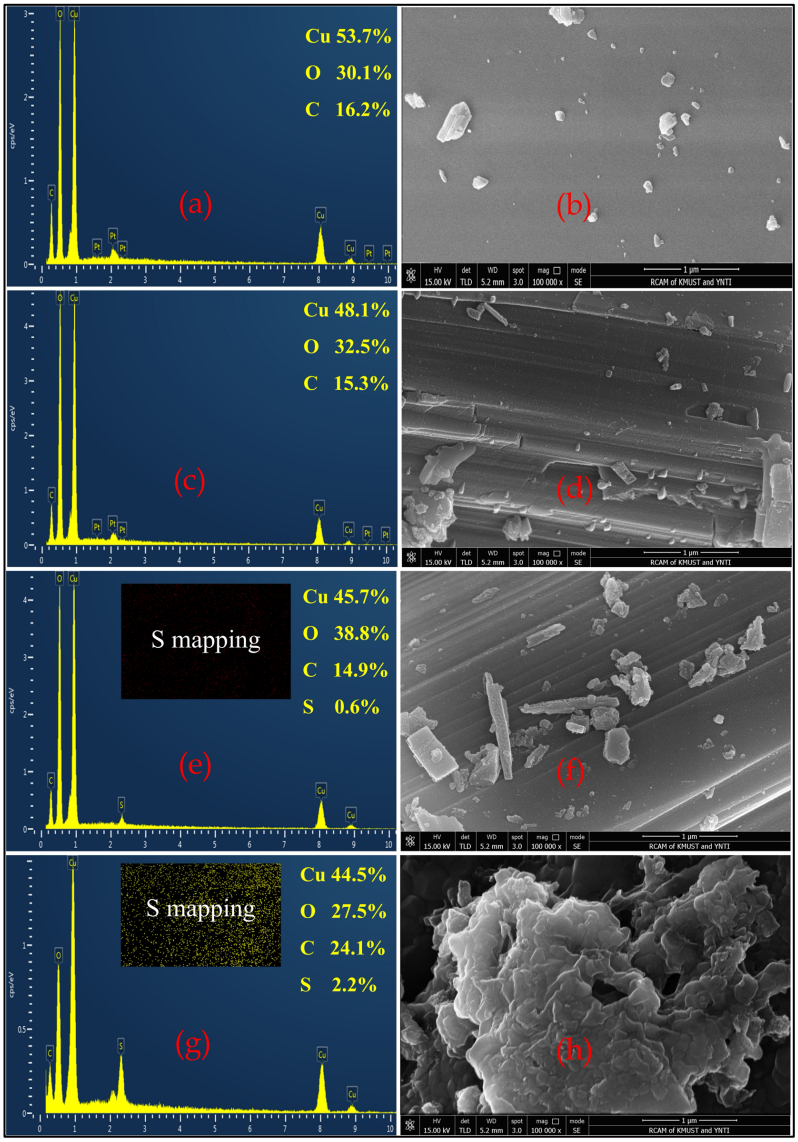


Fig. 6. FESEM-EDS results and proportions of Cu, S, C, and O of (a, b) pure malachite, (c, d) DDTC treatment, (e, f) $Na_2S$ treatment, and (g, h) $Na_2S$+DDTC treatment

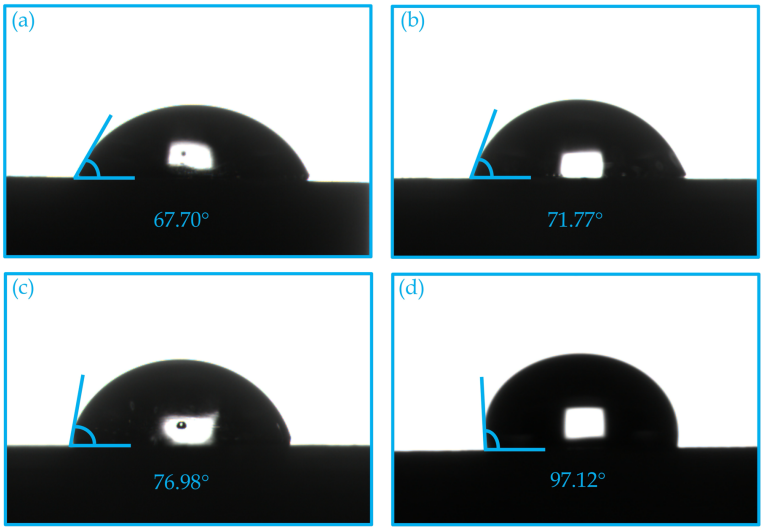


Fig. 7. Contact angle evolution of the malachite surface under various conditions: (a) pure malachite, (b) with DDTC, (c) with $Na_2S$, and (d) with $Na_2S$+DDTC+NaBX

### 3.7. Zeta potential analysis

The electrical double layer determines how flotation reagents adsorb onto the mineral-water interface (Fu et al., 2021). Pure malachite's isoelectric point (IEP) is pH = 8.7, consistent with previously published IEP values for malachite (Li et al., 2015; Liu et al., 2019, 2016; Zhang et al., 2021). At lower pH, malachite's surface is protonated ($-OH_2^+$), resulting in a positive charge. As the pH increases, deprotonation of hydroxyl groups ($-OH^-$) leads to a more negative surface charge. When a xanthate collector is introduced, the zeta potential crosses zero and shifts negative, indicating that xanthate ions ($RCSS^-$) adsorb onto the malachite surface. With the addition of DDTC and xanthate, xanthate likely adsorbs onto the malachite surface through physical and chemical mechanisms, increasing its presence on the mineral surface and causing a gradual decrease in zeta potential. Collector adsorption improves the stability of hydrophobic species. Adding sodium sulfide and xanthate further increases the negative surface potential. Sodium sulfide releases sulfur ions ($S^{2-}$), which bind to metal ions on the surface, forming metal sulfide complexes and enhancing the negative charge. This sulfurization process further promotes xanthate's negative charge through its ionic groups. After adding $Na_2S$ with DDTC and NaBX collectors, the zeta potentials became more negative across the tested pH range. This suggests that DDTC and NaBX interact with positively charged copper species on the malachite surface, promoting the formation of a Cu-S metal layer. The reaction between $Na_2S$ and the mineral creates a more negative surface potential, enhancing subsequent collector adsorption. The zeta potential stabilizes at pH > 8, indicating that DDTC or NaBX adsorption reduces the surface potential, as shown in Fig. 8.

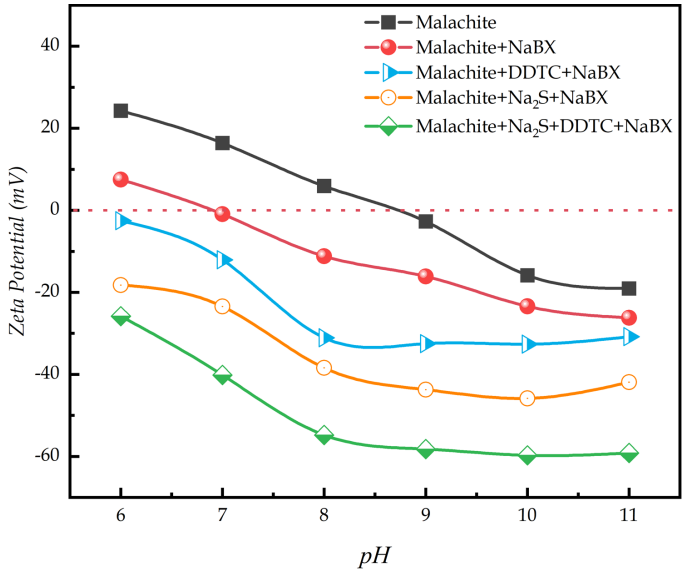


Fig. 8. Zeta potential graph of malachite at varying pH levels and in the presence of flotation reagents

### 3.8. FT-IR spectra analysis

Figs. 9(a, b) display the infrared spectra of the reagents $Na_2S$ and DDTC. FTIR spectra were obtained to compare the chemical behavior of the samples with these reagents. In the DDTC spectra, wide bands at 2849 $cm^{-1}$ and 2912 $cm^{-1}$ correspond to the symmetric C–H stretching of methyl and methylene groups (Mohammadi et al., 2020). The peak at 1695 $cm^{-1}$ is attributed to the bending vibration of O–H in crystallized water (Mohammadi et al., 2021). The peak at 1496 $cm^{-1}$ corresponds to C–N vibration in the N–C=S group (Touati and Meniai, 2012), while the peak range from 1257–1049 $cm^{-1}$ is due to C=S vibrations in the DDTC structure (Cordeiro et al., 2021). Peaks in the 1000–800 $cm^{-1}$ range indicate C–S vibrations (Mazur et al., 2019). In the $Na_2S$ spectra, the peak at 3416 $cm^{-1}$ is assigned to O–H stretching vibrations, likely from adsorbed water. Peaks at 2851 and 2917 $cm^{-1}$ are associated with C–H stretching, possibly due to minor hydrocarbon contamination. Peaks at 2523 and 2072 $cm^{-1}$ suggest weak S–H stretching, likely from hydrated or slightly oxidized $Na_2S$. Peaks at 1201 and 1260 $cm^{-1}$ correspond to sulfide oxidation products (S–O), resulting from sample oxidation over time. The peak at 1401 $cm^{-1}$ may indicate carbonate impurities ($CO_3^{2-}$), typically associated with symmetric C–O stretching. In the malachite spectrum, bands at 3404 and 3314 $cm^{-1}$ are attributed to O–H stretching vibrations, while the

strong bands at 1505 $cm^{-1}$ and 1497 $cm^{-1}$ correspond to C=O stretching within the carbonate ($CO_3^{2-}$) group (Fig. 10(a), (Wang et al., 2022). In the malachite + DDTC treatment spectrum, C–N, C=S, and C–S vibrational peaks appeared on the malachite surface between 1505 and 1046 $cm^{-1}$, indicating DDTC adsorption onto the malachite surface, consistent with the XPS results. This suggests that DDTC enhances malachite recovery by increasing surface hydrophobicity, as shown in Fig. 10(b).

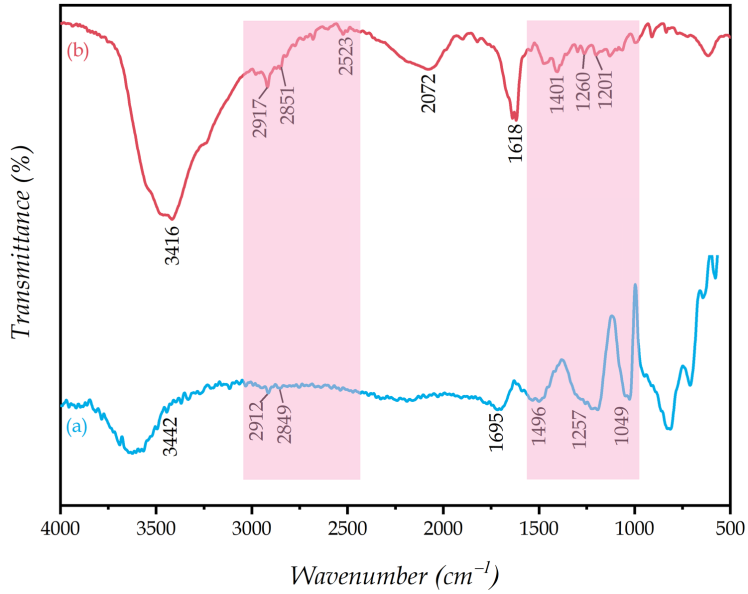


Fig. 9. FTIR spectra of (a) DDTC, (b) $Na_2S$

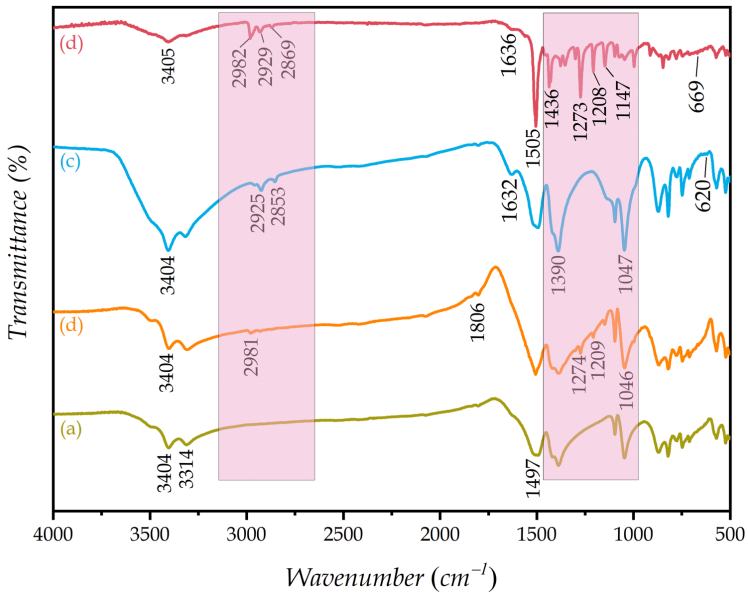


Fig. 10. FTIR spectra of (a) pure malachite, (b) with DDTC, (c) with $Na_2S$, and (d) with $Na_2S$+DDTC

After treatment with $Na_2S$, peaks in the 2925–2853 $cm^{-1}$ range correspond to C–H stretching, and those in the 1390–1047 $cm^{-1}$ range are related to C–O stretching and O–H bending vibrations. The peak at 1632 $cm^{-1}$ represents water molecules' H–O–H bending mode. A weak band at 620 $cm^{-1}$ is attributed to Cu–S stretching, confirming $Na_2S$ modification of the malachite surface (Q. Liu et al., 2020; Pei et al., 2011; Zhang et al., 2022), as shown in Fig. 10(c). In contrast, Fig. 10(d) shows that in the spectrum of malachite treated with both DDTC and $Na_2S$, the adsorption bands at 1505–1147 $cm^{-1}$, 1636 $cm^{-1}$, 2982–2869 $cm^{-1}$, and 3405 $cm^{-1}$ correspond to C–N and C–O stretching, H–O–H bending, C–H stretching, and O–H stretching vibrations, respectively. The addition of DDTC first forms active sites on the surface, promoting further sulfide adsorption. Sodium sulfide stabilizes a hydrophobic layer, enhancing

floatability and improving mineral recovery. Compared to direct sulfurization, the FTIR spectrum of malachite treated with both $Na_2S$ and DDTC shows a shift of the weak band to 669 $cm^{-1}$, indicating a modification of the Cu–S bond's chemical environment due to the combined treatment.

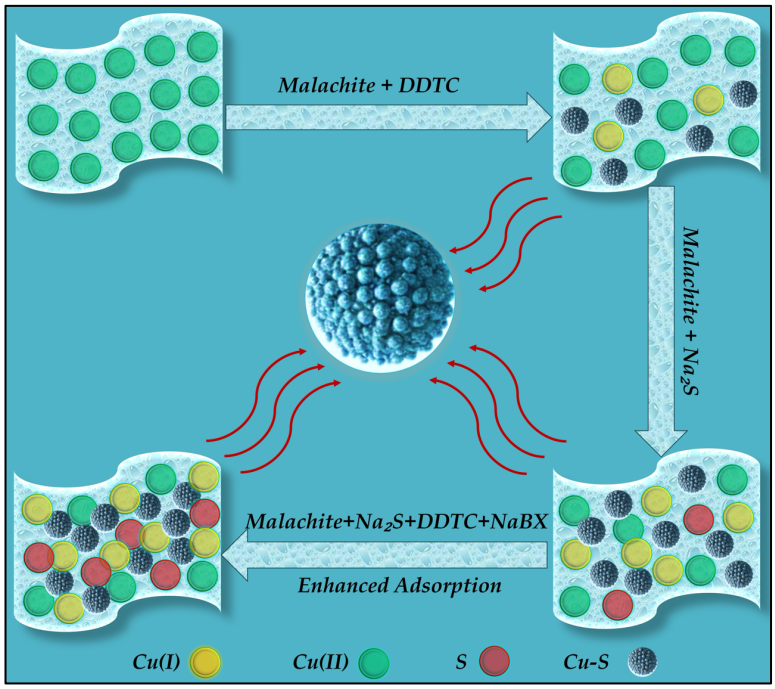


Fig. 11. Schematic of the collaborative collection mechanism of DDTC and xanthate in the sulfurization flotation process of malachite

Based on the calculations, DDTC and NaBX facilitate sulfur adsorption and reduce $Cu^{2+}$ to $Cu^{1+}$ on the malachite surface, forming copper(I) sulfide ($Cu_2S$). This sulfide layer significantly enhances the surface hydrophobicity of malachite, improving its flotation behavior. As shown in Fig. 11, the stages of DDTC-driven sulfurization are illustrated, emphasizing the role of these reagents in promoting efficient flotation. The hydrophobic $Cu_2S$-coated malachite particles more readily attach to air bubbles in the flotation cell, enhancing the separation of malachite from non-sulfurized gangue minerals and improving flotation efficiency. Consequently, malachite recovery is significantly increased, demonstrating the effectiveness of DDTC and NaBX in optimizing separation and enriching the concentrate through sulfurization.

## 4. Conclusion

This study used DDTC and NaBX collectors to improve the adsorption mechanism on malachite surfaces via sulfurization flotation, enhancing separation efficiency. Key conclusions are drawn from this work:

(1) The flotation experiments demonstrated optimal recovery at pH 9.0, achieving a maximum efficiency of 93.15% with both reagents combined. Increased flotation time and appropriate concentrations of $Na_2S$ and DDTC further enhanced recovery. However, excessively high concentrations reduced recovery due to precipitate formation, hindering flotation efficiency.

(2) The application of DDTC and NaBX as collectors in malachite sulfurization flotation enhanced recovery while increasing selectivity and yield by promoting copper ion conversion and improving mineral surface properties.

(3) The strong frontal redox reaction between $Cu^{2+}$ ions, DDTC, NaBX, and $Na_2S$ plays a key role in sulfurization, facilitating the formation and stability of Cu–S complexes, which enhances flotation efficiency.

(4) Infrared spectral analysis demonstrated that DDTC improved malachite sulfurization recovery by increasing surface hydrophobicity through the formation of C–N, C–S, and C=S bonds, which promoted the adsorption of xanthate ions.

**Acknowledgments**

This research project was supported by the Central Guidance Local Scientific and Technological Development Funds (202407AB110022), National Natural Science Foundation of China (Grant No. 52074138), Basic research project of Yunnan Province (Grant No. 202001AS070030 & 202201AU070099), and Yunnan Major Scientific and Technological Projects (Grant No. 202202AG050015).

**References**

AGRAWAL, A., SAHU, K.K., 2010. *Problems, prospects and current trends of copper recycling in India: An overview.* Resour. Conserv. Recycl. 54, 401–416.

ARNDT, N.T., FONTBOTÉ, L., HEDENQUIST, J.W., KESLER, S.E., THOMPSON, J.F.H., WOOD, D.G., 2017. *Future global mineral resources.* Geochemical Perspect. 6, 1–184. https://doi.org/10.7185/geochempersp.6.1

BAI, X., LIU, J., WEN, S., WANG, Y., LIN, Y., 2020. E*ffect of ammonium salt on the stability of surface sulfide layer of smithsonite and its flotation performance.* Appl. Surf. Sci. 514.

CHÁVEZ JR, W.X., 2021. *Weathering of copper deposits and copper mobility: Mineralogy, geochemical stratigraphy, and exploration implications.* SEG Newsl. 16–27.

CHEN, M., BAI, X., LI, W., LIU, J., SONG, M., LIU, Y., HAO, J., GAO, H., JIANG, M., 2025. *Study on the stability of malachite surface sulfide layer and the mechanism of ammonium salt-induced enhancement of sulfurization.* Sep. Purif. Technol. 360.

CORDEIRO, A.P., FEUSER, P.E., FIGUEIREDO, P.G., DA CUNHA, E.S., MARTINEZ, G.R., MACHADO-DE-ÁVILA, R.A., ROCHA, M.E.M., DE ARAÚJO, P.H.H., SAYER, C., 2021. *In vitro synergic activity of diethyldithiocarbamate and 4-nitrochalcone loaded in beeswax nanoparticles against melanoma (B16F10) cells.* Mater. Sci. Eng. C 120, 111651.

DONG, L., WEI, Q., QIN, W., JIAO, F., 2021. *Effect of iron ions as assistant depressant of citric acid on the flotation separation of scheelite from calcite.* Chem. Eng. Sci. 241, 116720.

FENG, Q., ZHAO, W., WEN, S., 2018. *Surface modification of malachite with ethanediamine and its effect on sulfidization flotation.* Appl. Surf. Sci. 436, 823–831.

FENG, Q., ZHAO, W., WEN, S., CAO, Q., 2017. *Copper sulfide species formed on malachite surfaces in relation to flotation.* J. Ind. Eng. Chem. 48, 125–132.

FU, Y. FENG, YIN, W. ZHONG, DONG, X. SHU, SUN, C. YAO, YANG, B., YAO, J., LI, H. LIANG, LI, C., KIM, H., 2021. *New insights into the flotation responses of brucite and serpentine for different conditioning times: Surface dissolution behavior.* Int. J. Miner. Metall. Mater. 28, 1898–1907.

GROZDANKA D. BOGDANOVIĆ, VELIZAR D. STANKOVIĆ, MAJA S. TRUMIĆ, DEJAN V. ANTIĆ, M.Ž.T., 2016. *Leaching of Low-grade Copper Ores: A case Study For „Kraku Bugaresku-Cementacija" Deposits (Eastern Serbia).* J. Min. Metall. 52, 45–56.

GUPTA, A.N., KUMAR, V., SINGH, V., RAJPUT, A., PRASAD, L.B., DREW, M.G.B., SINGH, N., 2015. *Influence of functionalities on the structure and luminescent properties of organotin(IV) dithiocarbamate complexes.* J. Organomet. Chem. 787, 65–72.

GUPTA, A.N., SINGH, V., KUMAR, V., RAJPUT, A., SINGH, L., DREW, M.G.B., SINGH, N., 2013. *Syntheses, crystal structures and conducting properties of new homoleptic copper (II) dithiocarbamate complexes*. Inorganica Chim. Acta 408, 145–151.

IBRAHIM, A.M., JIA, X., CAI, J., SU, C., YU, X., ZHENG, Q., PENG, R., SHEN, P., LIU, D., 2023. *Role of ammonium phosphate in improving the physical characteristics of malachite sulfidation flotation.* Physicochem. Probl. Miner. Process. 59, 1–13.

IBRAHIM, A.M., JIA, X., SU, C., CAI, J., SHEN, P., LIU, D., 2022. *Effect of Ammonium Sulfide on Sulfidization Flotation of Malachite.* Minerals 12, 1–14.

IBRAHIM, A.M., WANG, H., YOUSIF, J.A., ELHADI, M., SHEN, P., LIU, D., 2025. *Improved activation of malachite sulfurization flotation by thiourea's (CS(NH2)2): Performance and mechanism study.* Colloids Surfaces A Physicochem. Eng. Asp. 705, 135643.

JIA, X. DONG, SONG, K. WEI, CAI, J. PENG, SU, C., XU, X. HUI, MA, Y. YU, SHEN, P. LUN, LIU, D. WEN, 2023. *Effect of oxygen and sodium sulfide on flotation of cuprite and its modification mechanism.* Trans. Nonferrous Met. Soc. China (English Ed. 33, 1233–1243.

LI, F., ZHONG, H., XU, H., JIA, H., LIU, G., 2015. *Flotation behavior and adsorption mechanism of a-hydroxyoctyl phosphinic acid to malachite.* Miner. Eng. 71, 188–193.

LI, Q., HUANG, L., HU, B., HUANG, S., ZHOU, J., XU, Y., 2025. *Synthesis and utilization of a novel amidoxime collector for the flotation separation of cuprite from calcite.* Sep. Purif. Technol. 353.

LI, Z., RAO, F., ESCUDERO GARCÍA, R., LI, H., SONG, S., 2018. *Partial replacement of sodium oleate using alcohols with different chain structures in malachite flotation.* Miner. Eng. 127, 185–190.

LIAO, R., WEN, S., LIU, J., BAI, S., FENG, Q., 2024. *Experimental and molecular dynamics simulation study on DDA/DDTC mixed collector co-adsorption on sulfidized smithsonite surfaces.* Miner. Eng. 205, 108493.

LIU, C., SONG, S., LI, H., LI, Y., AI, G., 2019. *Elimination of the adverse effect of calcite slimes on the sulfidization flotation of malachite in the presence of water glass.* Colloids Surfaces A Physicochem. Eng. Asp. 563, 324–329.

LIU, C., ZHU, G., SONG, S., LI, H., 2018. *Interaction of gangue minerals with malachite and implications for the sulfidization flotation of malachite.* Colloids Surfaces A Physicochem. Eng. Asp. 555, 679–684.

LIU, G., HUANG, Y., QU, X., XIAO, J., YANG, X., XU, Z., 2016. *Understanding the hydrophobic mechanism of 3-hexyl-4-amino-1, 2,4-triazole-5-thione to malachite by ToF-SIMS, XPS, FTIR, contact angle, zeta potential and micro-flotation.* Colloids Surfaces A Physicochem. Eng. Asp. 503, 34–42.

LIU, M., CHEN, D., HU, B., HE, P., CHEN, Y., ZENG, H., ZHANG, C., ZHU, J., 2024. *New insights into the activation mechanism of ammonium ions on the malachite sulfidization flotation.* Miner. Eng. 205.

LIU, Q., ZHANG, S., XU, Y., 2020. *Two-step synthesis of CuS/C@PANI nanocomposite as advanced electrode materials for supercapacitor applications.* Nanomaterials 10, 1034.

LIU, R., LIU, D., LI, JIALEI, LI, JIANMIN, LIU, Z., JIA, X., YANG, S., LI, JIANGLI, NING, S., 2020. *Sulfidization mechanism in malachite flotation: A heterogeneous solid-liquid reaction that yields CuxSy phases grown on malachite.* Miner. Eng. 154.

LU, W., WEN, S., LIU, D., WANG, H., FENG, Q., 2023. *A novel method for improving sulfidization xanthate flotation of malachite: Copper–ammonium synergistic activation*. Appl. Surf. Sci. 618, 156660.

MAJUMDAR, D., GHOSH, S., 2021. *Recent advancements of copper oxide based nanomaterials for supercapacitor applications.* J. Energy Storage 34, 101995.

MALEKI, H., NOAPARAST, M., CHEHREGHANI, S., MIRMOHAMMADI, M.S., REZAEI, A., 2023. *Optimization of flotation of the Qaleh Zari mine oxidized copper ore sample by the sequential sulfidation approach using the response surface method technique.* Rud. Geol. Naft. Zb. 38, 59–68.

MAZUR, K.L., FEUSER, P.E., VALÉRIO, A., POESTER CORDEIRO, A., DE OLIVEIRA, C.I., ASSOLINI, J.P., PAVANELLI, W.R., SAYER, C., ARAÚJO, P.H.H., 2019. *Diethyldithiocarbamate loaded in beeswax-copaiba oil nanoparticles obtained by solventless double emulsion technique promote promastigote death in vitro.* Colloids Surfaces B Biointerfaces 176, 507–512.

MOHAMMADI, I., SHAHRABI, T., MAHDAVIAN, M., IZADI, M., 2021. *Chemical modification of LDH conversion coating with diethyldithiocarbamate as a novel anti-corrosive film for AA2024-T3*. J. Ind. Eng. Chem. 95, 134–147.

MOHAMMADI, I., SHAHRABI, T., MAHDAVIAN, M., IZADI, M., 2020. *Cerium/diethyldithiocarbamate complex as a novel corrosion inhibitive pigment for AA2024-T3*. Sci. Rep. 10, 1–15.

MUSTAFA, S., HAMID, A., NAEEM, A., 2004. *Xanthate adsorption studies on chalcopyrite ore.* Int. J. Miner. Process. 74, 317–325.

NIKITHA, M., SOWNDHARYA, S., MEENAKSHI, S., 2024. *Assessment of visible light sensitive La-doped BiOBr/ZnO for the effective degradation of malachite green dye.* J. Water Process Eng. 63, 105571.

NORTHEY, S., MOHR, S., MUDD, G.M., WENG, Z., GIURCO, D., 2014. *Modelling future copper ore grade decline based on a detailed assessment of copper resources and mining*. Resour. Conserv. Recycl. 83, 190–201.

PEI, L.Z., WANG, J.F., TAO, X.X., WANG, S.B., DONG, Y.P., FAN, C.G., ZHANG, Q.F., 2011. *Synthesis of CuS and Cu1.1Fe1.1S2 crystals and their electrochemical properties.* Mater. Charact. 62, 354–359.

RÖTZER, N., SCHMIDT, M., 2020. *Historical, current, and future energy demand from global copper production and its impact on climate change.* Resources 9.

SAID, Z., SOHAIL, M.A., WALVEKAR, R., LIU, C., 2022. *Impact of sonication durations on thermophysical properties, contact angle and surface tension of f-MWCNTs nanofluid for heat transfer*. J. Mol. Liq. 358, 119164.

TÉLLEZ S., C.A., COSTA, A.C., MONDRAGÓN, M.A., FERREIRA, G.B., VERSIANE, O., RANGEL, J.L., LIMA, G.M., MARTIN, A.A., 2016. *Molecular structure, natural bond analysis, vibrational and electronic spectra, surface enhanced Raman scattering and Mulliken atomic charges of the normal modes of [Mn(DDTC)2] complex. Spectrochim.* Acta - Part A Mol. Biomol. Spectrosc. 169, 95–107.

TOUATI, S., MENIAI, A.H., 2012. *Solvent extraction of Cu (II) from sulphuric acid by means of sodium diethyldithiocarbamate and characterization of the formed complex*. Theor. Found. Chem. Eng. 46, 719–726.

WANG, C., SUN, L., WANG, Q., WANG, Y., CAO, Y., WANG, X., CHEN, P., SUN, W., 2022. *Adsorption mechanism and flotation behavior of ammonium salt of N-Nitroso-N-phenylhydroxyamine on malachite mineral*. Appl. Surf. Sci. 583, 152489.

WU, D., MAO, Y., DENG, J., WEN, S., 2017. *Activation mechanism of ammonium ions on sulfidation of malachite (–201) surface by DFT study*. Appl. Surf. Sci. 410, 126–133. h

XIAO, W., ZHANG, Z., YANG, J., ZHAO, Y., LAI, C., WANG, H., WANG, Q., FANG, J., YANG, S., 2024. *Flotation separation mechanism of malachite from calcite using the pentyl xanthate as the collector*. Miner. Eng. 206, 108540.

XUE, J., QU, Y., CHEN, Y., ZHANG, C., BU, X., 2023. *Effective sulfide flotation of cerussite by using trithiocyanuric acid as a novel sulfurizing reagent*. Miner. Eng. 198, 108087.

YU, X., SHEN, P., YIN, Z., WANG, L., WANG, H., LIU, D., 2023. *Surface modification of malachite using DMTD and its effect on xanthate adsorption.* Colloids Surfaces A Physicochem. Eng. Asp. 679, 132560.

ZHANG, C., ZHOU, Q., AN, B., YUE, T., CHEN, S., LIU, M., HE, J., ZHU, J., CHEN, D., HU, B., SUN, W., 2021. *Flotation behavior and synergistic mechanism of benzohydroxamic acid and sodium butyl-xanthate as combined collectors for malachite beneficiation*. Minerals 11, 1–16.

ZHANG, H., ZHOU, Q., LIN, S., ZHANG, C., SUN, W., CHEN, D., WANG, R., LIU, M., CHEN, J., 2022. *Surface modification of malachite with tetraamminecopper (II) and its effect on sulfidation flotation*. Miner. Eng. 189, 107882.

ZHANG, Q., WANG, Y., FENG, Q., WEN, S., ZHOU, Y., NIE, W., LIU, J., 2020. *Identification of sulfidization products formed on azurite surfaces and its correlations with xanthate adsorption and flotation*. Appl. Surf. Sci. 511, 145594.

ZHANG, Y., CAO, Z., CAO, Y., SUN, C., 2013. *FTIR studies of xanthate adsorption on chalcopyrite, pentlandite and pyrite surfaces*. J. Mol. Struct. 1048, 434–440.

ZUO, Q., WU, D., WEN, S., CHEN, H., CAO, J., 2024. *Surface activation of malachite by ammonium acetate for improved flotation separation of malachite from calcite*. Appl. Surf. Sci. 642, 158606.